Mechanical Evaluation and XRD/TG Investigation on the Properties of Wooden Dowel Welding

Xudong Zhu,[a,b,c] Songlin Yi,[a,,b,c]* Ying Gao,[a,b,c] Yuting Zhao,[a,b,c] and Yaqin Qiu [a,b,c]

Mechanical properties related to wooden dowel welding were studied using five different moisture content (MC) values. Birch wooden dowels and Chinese larch substrates were used in this study. A 2% MC for the wooden dowels and a 12% MC for the substrates resulted in the highest pullout resistance. A fitting analysis showed that there was a linear relationship between the pullout resistance and the different values of MC. The errors between the calculated values and the test values were less than 10%. The pullout resistance of the wooden dowel welding fit a Weibull distribution. No accurate linear relation existed between the 95% reliability pullout resistance and the different MC values. Chemical analyses were performed separately on the wooden dowel and the welding interface of a wooden dowel sample with 2% MC and a substrate with 12% MC. X-ray diffraction (XRD) analysis revealed that the degree of crystallinity of the welding interface was 75% higher than that of the wooden dowel. Finally, thermogravimetric analysis (TG) illustrated that pyrolysis of the wood components occurred during the wooden dowel welding process.

Keywords: Wooden dowel welding; Pullout resistance; Linear relation; Weibull distribution; Pyrolysis

*Contact information: a: Beijing Key Laboratory of Wood Science and Engineering, Beijing Forestry University, Beijing 100083, China; b: Ministry of Education Key laboratory of Wooden Material Science and Application, Beijing Forestry University, Beijing 100083, China; c: Ministry of Education Engineering Research Center of Forestry Biomass Materials and Bioenergy, Beijing Forestry University, Beijing 100083, China; *Corresponding author: toyisonglin@gmail.com*

INTRODUCTION

Rotational welding technology is a new research direction in the field of forming wooden connections without adhesives. This approach creates a new bonding interface layer utilizing the friction between the wooden dowels and substrate holes. During this process, some wood components are softened, fused, and eventually become solidified until the friction stops. The main components of wood are natural polymers of cellulose, hemicellulose, and lignin. Cellulose is relatively stable, hemicellulose generates thermal pyrolysis, and lignin depolymerizes and softens during the welding process (Sandberg *et al*. 2013; Zhou *et al*. 2014).

The dowel/hole diameter difference, wood grain direction, dowel moisture content, and type of wood species all contribute to weld properties. Kanazawa *et al.* (2005) found that substrate holes with different diameters at different depths could improve the pullout resistance. The pullout resistance of the welded joints oriented normal to the grain (Fig. 1) was higher than that of joints oriented along the end grain (Fig. 2). Dry dowels also improve the pullout resistance due to the swelling associated with the equilibrium moisture content, created by the absorption of water from the environment (Kanazawa *et al.* 2005). Wood species also alter the process, and Belleville reported better pullout resistance of sugar maple compared to that of yellow birch (Belleville *et al.* 2013b).

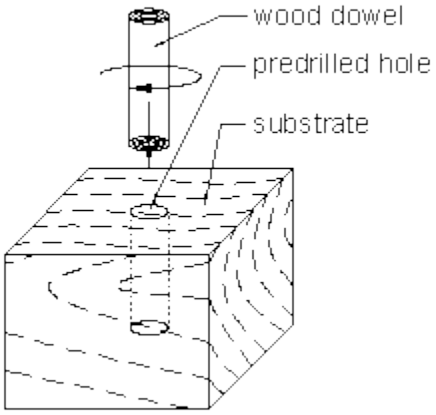

Fig. 1. Wooden dowel welded into a predrilled hole normal to the grain

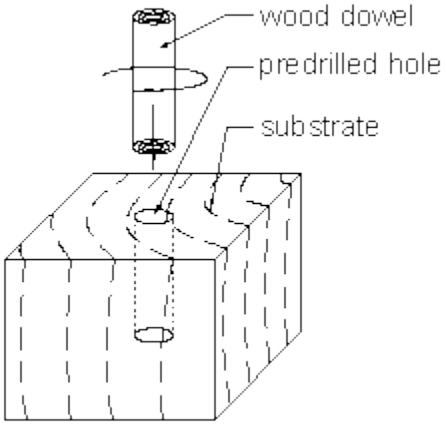

Fig. 2. Wooden dowel welded into a predrilled hole along the grain

In other studies, rotational and insertion speed have been shown to play an important role in the weld strength. According to Leban *et al.* (2008), the pullout resistance of welded joints was 2145 N at a rotational speed of approximately 1500 rpm and a weld depth of 22 mm. Pullout resistance in the range of 2500 N to 2550 N at a 46 mm depth insertion was not significantly affected by the rotational speed (Leban *et al*. 2008). Meanwhile, Leban found that the optimum rotational speed was 1000 rpm due to the occurrence of charring at higher rotation speeds for sugar maple and yellow birch. The weld properties using a constant insertion speed and a high rotational speed were better than the properties when an accelerating speed was used (Auchet *et al*. 2010). Because of this trend, the best constant insertion speeds for sugar maple and yellow birch were 25 mm/s and 16.7 mm/s, respectively (Belleville *et al*. 2013b). In the welded joints, the interface materials were determined to primarily come from the wooden dowels (Rodriguez *et al*. 2010).

An analysis of the interactions between the welding parameters was performed by Canne *et al.* (2005). Their study showed that the rotation rate/dowel moisture content was the most significant under several combinations, including rotation rate/dowel temperature, wood grain direction/wood species, and dowel temperature/wood species (Ganne-Chedeville *et al*. 2005).

The dowel welding process was monitored using a thermal camera and observed to reach temperatures as high as 180 °C, before decreasing to 60 °C to 70 °C in less than 1

min (Kanazawa *et al.* 2005). Although this process produced a welded joint with satisfactory strength, the production of furanic aldehydes was high, as determined by solid-state 13C-NMR analysis. At higher dowel insertion speed, the production of furanic aldehydes also increased and xylans and lignin comprised most of the flowing material (Kanazawa *et al*. 2005). Recrystallised xylans and furanic compounds were generated from the pyrolysis of the carbohydrates (Pizzi *et al*. 2006). The smoke generated by the welding process was composed of water vapour, carbon dioxide, and other nontoxic volatile degradation compounds (Omrani *et al*. 2008).

As described above, many studies have investigated the influence of wooden dowel moisture content. However, the interaction influence of wooden dowel and substrate moisture content has not been evaluated. Here, regression analysis was performed to determine the relationship between pullout resistance and the different MC values. The Weibull distribution was applied to study the pullout resistance, and the 0.05 fractile of pullout resistance was calculated. Additionally, we evaluated the performance of wooden dowel welding using previously described methods (Delmotte *et al*. 2008; Segovia and Pizzi 2009; Belleville *et al*. 2013a) to measure the degree of crystallinity using an X-ray diffractometer (XRD) and to detect chemical changes using thermogravimetric analysis (TG).

EXPERIMENTAL

Materials

Wooden dowels, 12 mm in diameter and 100 mm in length, were fabricated from birch (*Betula pendula*) and had an average density of 557 kg/m^3. Chinese larch (*Larix gmelinii*) slats with an average density of 680 kg/m^3 were used as substrates with dimensions of 40 mm (Tangential) × 50 mm (Radial) × 500 mm (Longitudinal).

One-hundred pieces of wooden dowels and substrates were placed in an oven at 63 °C until 2% and 7% MC were reached, respectively. The temperature of 63 °C was selected based on preliminary experiments that showed that incubation at this temperature allowed the wooden dowels and substrates to achieve the desired MC over two days with little warping and cracking. Separately, 100 pieces of wooden dowels and substrates were exposed to a temperature of 20 °C and a relative humidity (RH) of 60% until reaching an equilibrium moisture content (EMC) of 12%. 20 pieces of substrates were placed in an oven at 100 °C until reaching 2% MC. All the five test groups were designed at Table 1.

Specimens prepared

According to the research of Leban, wood substrates were pre-drilled with holes 8.5 mm in diameter and 30 mm in depth using a drilling machine (Proxxon TBH Typ 28 124, Proxxon, Stuttgart, Germany). Next, the wooden dowels were welded into the pre-drilled holes in the substrates to create bonded joints, using a high-speed rotation rate of 1080 rpm and a feed rate of 10 mm/s (Fig. 1) (Leban *et al*. 2008). The inserted part of the dowel became conical in shape (Fig. 3) because of the different abrasion levels during the welding process. The rotation of the wooden dowel stopped when the fusion and bonding was achieved in approximately 2 to 4 s (Belleville *et al*. 2013b). The specimens that had been manufactured with different MC values are shown in Table 1.

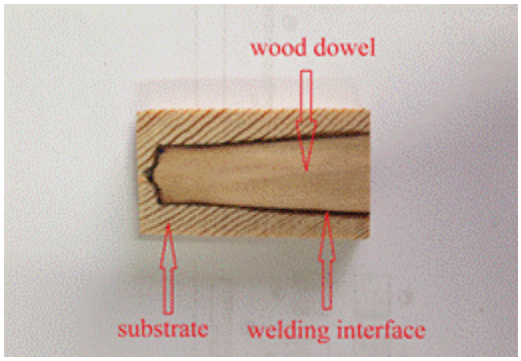

Fig. 3. The conical shape of the welding interface

Methods

Pullout resistance test

After welding, the wood slats were cut into 10 parts of equal length, so that every welded dowel was 40 mm (T) × 50 mm (R) × 50 mm (L) in size. The specimens were conditioned at 20 °C and 60% RH for seven days before the tests were conducted.

Fig. 4. The WDW-300E universal testing equipment

The pullout resistance of the specimens was tested using a universal testing machine (WDW-300E, Fig. 4, Jinan Popwil, Shandong, China) that pulled the welded wooden dowels out of the substrate at a speed of 2 mm/min (O'Loinsigh *et al*. 2012). The specimens were fixed by clamping the dowel into the jaw of the fixed beam, while the substrate block was fixed to the crosshead of the machine *via* a metallic grip.

Weibull distribution analyses

The Weibull distribution function $F(x)$ was determined according to Eq. 1,

$$F(x) = 1 - e^{-\left(\frac{x-a_0}{\beta}\right)^{\alpha}} \quad (1)$$

and the probability density function $f(x)$ was calculated according to Eq. 2, which was transformed by a differential of Eq. 1,

$$f(x)=\frac{\alpha}{\beta}\times\left(\frac{x-a_0}{\beta}\right)^{\alpha-1}\times e^{-\left(\frac{x-a_0}{\beta}\right)^{\alpha}} \quad (2)$$

where α, β, and a_0 present the shape parameter, scale parameter, and location parameter, respectively. The variable x is the pullout resistance and $e^{-\left(\frac{x-a_0}{\beta}\right)^{\alpha}}$ is the probability of the random pullout resistance bigger than x.

Samples Prepared for XRD and TG Analyses

As shown in Table 1, Group D with a wooden dowel of 2% MC and a substrate of 12% MC showed the best pullout resistance; therefore, XRD and TG tests were performed on group D.

To determine the degree of crystallinity, XRD analyses were performed in a TWIST-TUBE X-ray diffractometer (Bruker D8 ADVANCE, Bruker, Karlsruhe, Germany) using Cu Kα radiation (40 kV, 200 mA), from 5° to 40°, with a step size of 8°/min. Two samples were prepared for the XRD test including a wooden dowel and a welding interface. Each sample was prepared by scraping and mixing the powders from all the 44 tested specimens in a uniform manner.

The programmed heating pyrolysis of the wooden dowel and welding interface was performed in a NETZSCH STA 449F3 simultaneous thermal analyzer (Netzsch, Freistaat Bayern, Germany). The samples in the TG crucible were heated from 323 K to 973 K at a heating rate of 10 K/min^{-1}. Purified nitrogen was used as the carrier gas to provide an inert atmosphere. The two samples were similarly prepared for XRD analyses. The TG analyses were performed using 10 mg powders for each test (Hu *et al*. 1998; Tan *et al*. 2006).

RESULTS AND DISCUSSION

Relationship between Pullout Resistance and Different MC Values

In order to assess the effect of different MC values on pullout resistance, the pullout resistances of the welded specimens are summarized in Table 1. Group D showed the best pullout resistance with 12% and 2% MC of substrates and wooden dowels, respectively. Group E showed the worst pullout resistance with 2% and 12% MC of substrates and wooden dowels, respectively. The typical fracture surface and the pullout resistance-displacement curve are shown in Fig. 5 and 6. From the data in Fig. 6, the rupture mode of the welded joint was considered a brittle rupture.

Fig. 5. The typical fracture surface of the welded joint

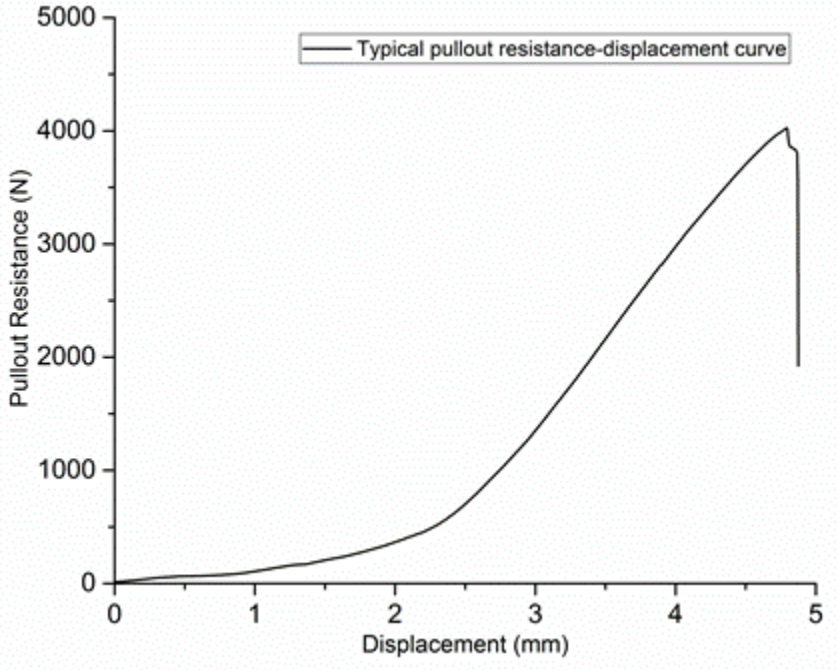

Fig. 6. Typical pullout resistance-displacement curve of the welded joint

Table 1. Pullout Resistance of Welded Specimens with Different Manufactured MC

Group	MC of Substrates (%)	MC of Wooden dowels (%)	Max. Value (N)	Min. Value (N)	Mean Value (N)	COV[2] (%)	Replicate Specimens
A	7	2	4616	1450	2867(740)[1]	25.81	52
B	7	12	2154	894	1487(331)[1]	22.26	27
C	12	12	3765	1261	2459(565)[1]	22.98	59
D	12	2	5307	2351	4027(649)[1]	16.12	44
E	2	12	948	524	786(141) [1]	17.96	15

Note: [1] -Parenthesis values are the standard deviation; [2] COV- Coefficient of Variation

The variation tendency of the pullout resistance with different MC values was studied. As shown in Fig. 7, the different MC values of the wooden dowels and substrates were set to the x-coordinate. For example, -10 was the difference value between the 2% and 12% MC of wooden dowels and substrates. With the increase in MC value difference, the pullout resistance showed a negative trend. Based on the analyses of linear fit performed using the Origin 10.1 software (OriginLab, Massachusetts, America), the linear relation could be inferred.

$$Y = -157.48X + 2324 \qquad (-10 \le X \le 10) \tag{3}$$

Based on the F-method of inspection, a test of significance of the linear relationship was next performed, where U and Q were the regression and residual sum of squares, respectively. When the level of significance was $\alpha = 0.05$, the $F_{1-\alpha}(1, 3) = 10.1$. According to Eq. 3, $U = 6181104$ and $Q = 98206$ were calculated, and then,

$$F = (n-2) \times \frac{U}{Q} = 3 \times \frac{6181104}{98206} = 1888 > 10.1 \tag{4}$$

The result of Eq. 4 indicates that a significant linear relationship exists between the pullout resistance and different MC values.

With the use of Eq. 3, the differences between the calculated values and test values are shown in Table 2. The errors of the five groups were less than 10%. This linear fit analysis showed a linear relationship between the pullout resistance and the different MC values. This relationship could be used to predict the pullout resistance with other MC conditions in future research.

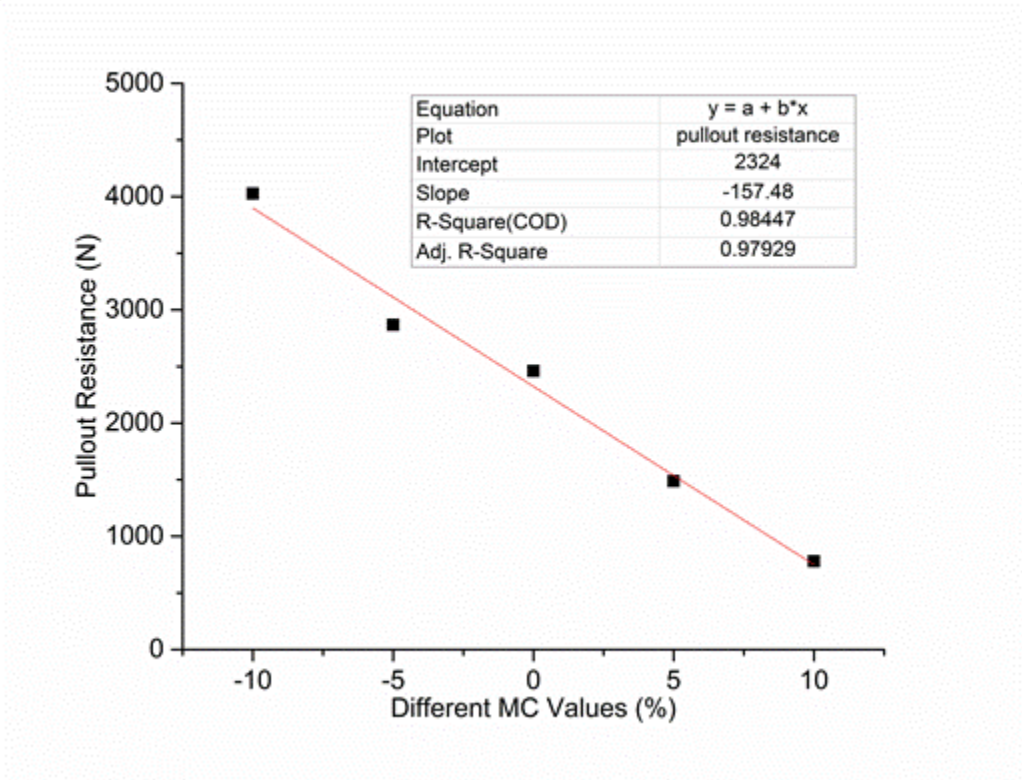

Fig. 7. Linear relation between the pullout resistance and different MC values

Table 2. Difference between the Calculated and Tested Pullout Resistance values

Group	Calculated Value (N)	Test Value (N)	Error (%)
A	3111.4	2867	7.86
B	1536.6	1487	3.23
C	2324.0	2459	5.81
D	3898.8	4027	3.29
E	749.2	786	4.91

Weibull Distribution of Pullout Resistance

For the brittle rupture of the welded joints during the resistance tests in this study, $a_0 = 0$ was assumed. Because there is discontinuity of the welding interface, pullout resistance with 0 N is reasonable (He *et al.* 2001; Yi 2002; Zheng *et al*. 2012). The Weibull distribution function should then be rewritten as follows:

$$1-F(x)=e^{-\left(\frac{x}{\beta}\right)^{\alpha}} \tag{5}$$

Once the logarithm of each side of the equation is taken, Eq. 5 can be rewritten as

$$\ln\left[-\ln\left(1-F(x)\right)\right]=\alpha\ln x-\alpha\ln\beta \tag{6}$$

In the Weibull distribution probability graph, ln x and ln[-ln(1-$F(x)$)] are set as the X-coordinate and Y-coordinate, respectively. Then, Eq. 6 could be rewritten as the linear Eq. 7. In this equation, $b = a$ and $a = -a$ ln β.

$$Y = bX + a \tag{7}$$

For the five welded groups, five equations were set, respectively.

$$Y = 4.2149X - 4.8385 \quad \text{(Group A)} \tag{8}$$

$$Y = 4.753X - 2.3001 \quad \text{(Group B)} \tag{9}$$

$$Y = 4.9921X - 4.9798 \quad \text{(Group C)} \tag{10}$$

$$Y = 6.603X - 9.6515 \quad \text{(Group D)} \tag{11}$$

$$Y = 5.3306X + 0.857 \quad \text{(Group E)} \tag{12}$$

Based on Eqs. 8 through 12, the parameters α and β were calculated, and are shown in Table 3. The table is followed by equations of the cumulative distribution and the probability density distribution for each group.

Table 3. Parameters α and β of the Five Welded Groups

Group	α	β
A	4.2149	3.1517
B	4.7530	1.6224
C	4.9921	2.7116
D	6.6030	4.3132
E	5.3306	0.8570

Group A:

$$F(x) = 1 - e^{-\left(\frac{x}{3.1517}\right)^{4.2149}} \quad (13)$$

$$f(x) = 1.33734 \times \left(\frac{x}{3.1517}\right)^{3.2149} \times e^{-\left(\frac{x}{3.1517}\right)^{4.2149}} \quad (14)$$

Group B:

$$F(x) = 1 - e^{-\left(\frac{x}{1.6224}\right)^{4.753}} \quad (15)$$

$$f(x) = 2.92961 \times \left(\frac{x}{1.6224}\right)^{3.753} \times e^{-\left(\frac{x}{1.6224}\right)^{4.753}} \quad (16)$$

Group C:

$$F(x) = 1 - e^{-\left(\frac{x}{2.7116}\right)^{4.9921}} \quad (17)$$

$$f(x) = 1.84102 \times \left(\frac{x}{2.7116}\right)^{3.9921} \times e^{-\left(\frac{x}{2.7116}\right)^{4.9921}} \quad (18)$$

Group D:

$$F(x) = 1 - e^{-\left(\frac{x}{4.3132}\right)^{6.603}} \quad (19)$$

$$f(x) = 1.53088 \times \left(\frac{x}{4.3132}\right)^{5.603} \times e^{-\left(\frac{x}{4.3132}\right)^{6.603}} \quad (20)$$

Group E:

$$F(x) = 1 - e^{-\left(\frac{x}{0.857}\right)^{5.3306}} \quad (21)$$

$$f(x) = 6.22007 \times \left(\frac{x}{0.857}\right)^{4.3306} \times e^{-\left(\frac{x}{0.857}\right)^{5.3306}} \quad (22)$$

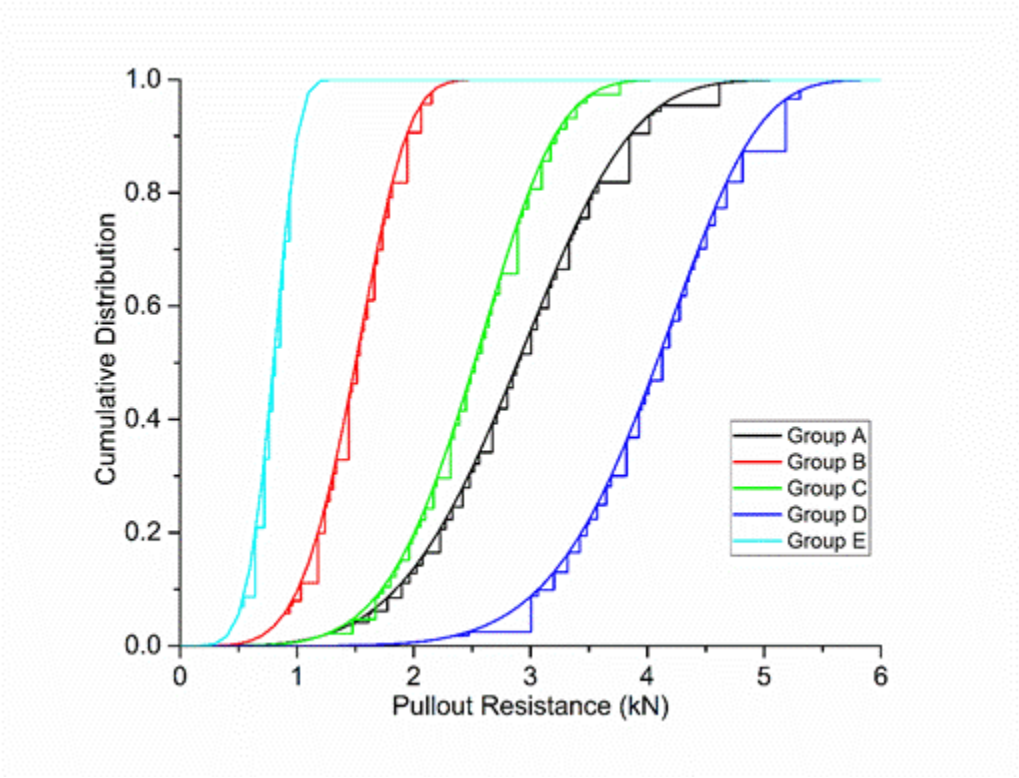

Fig. 8. Cumulative distribution of pullout resistance

Table 4. 0.05 Fractile of Pullout Resistance of Each Group

Group	0.05 Fractile of Pullout Resistance (N)
A	1558
B	869
C	1496
D	2751
E	491

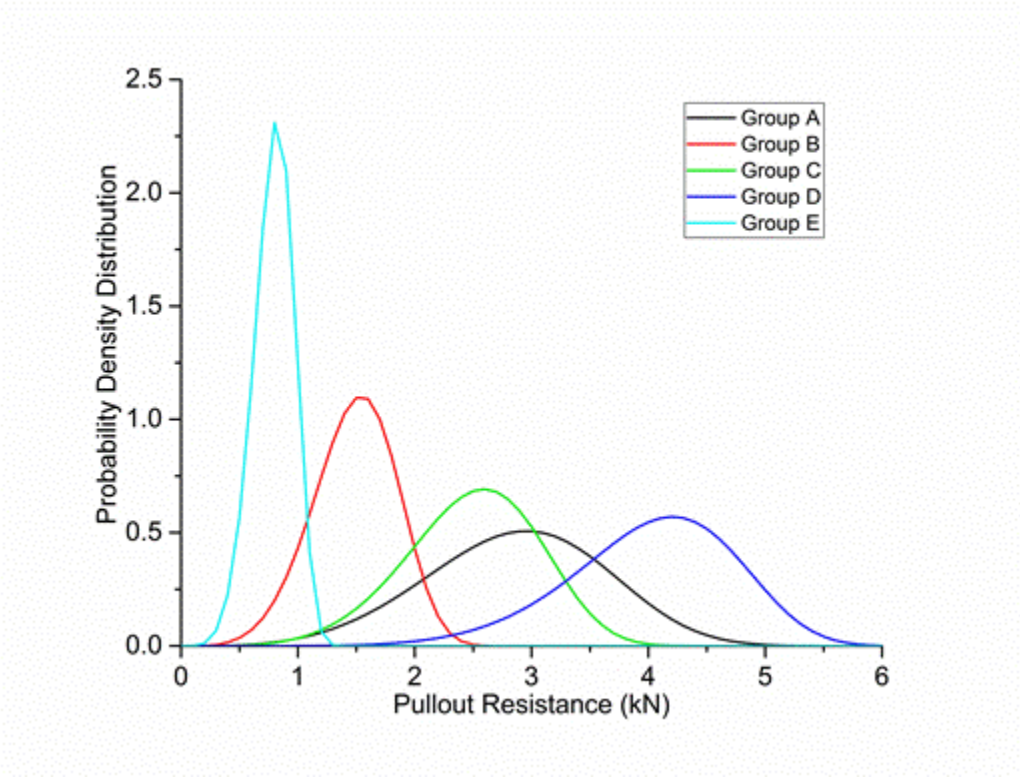

Fig. 9. Probability density distribution of pullout resistance

The data for all groups are shown in Figs. 8 and 9. In Fig. 8, the pullout resistances for five welded groups complied with the Weibull distribution. Therefore, the Weibull distribution could reasonably be used for the analysis of wooden dowel welding. In the furniture and construction industries, design values are applied. For connected joints, the design value corresponds to a 0.05 fractile value. From the data shown in Figs. 8 and 9, the 0.05 fractile of pullout resistance could be calculated (Table 4). Using the same linear fit analyses for pullout resistance, Fig. 10 shows the linear relation between the 0.05 fractile of pullout resistance and different MC values. The red line and Eq. 23, shows the linear relation for the data.

$$Y = -104.18X + 1433 \quad (23)$$

Based on the F-method of inspection, according to Eq. 23, U = 1665456 and Q = 248809.9; then $F = 3 \times \frac{U}{Q} = 20.1 > 10.1$, indicating a significant linear relationship. However, the linear relationship did not fit the data points accurately, especially at the -5 and 10 of X-coordinate. The errors between the calculated value and the test value at the -5 and 10 point of the X-coordinate were 20.26% and 25.51%, respectively.

The analyses may suggest a linear relationship between the 0.05 fractile of pullout resistance and different MC values. This should be considered more extensively by testing additional MC conditions in future research.

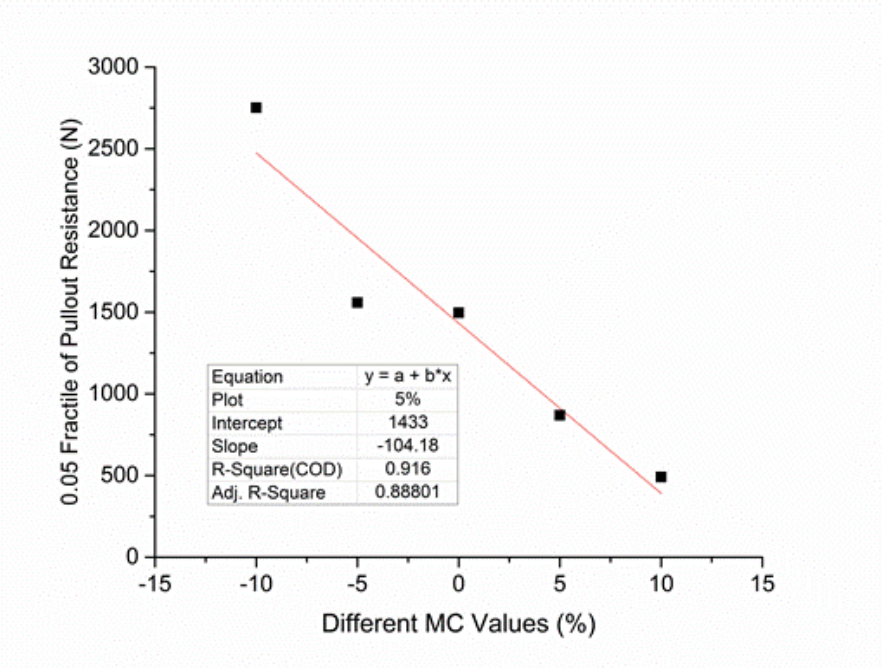

Fig. 10. Linear relation between the 0.05 fractile of pullout resistance and different MC values

XRD Analyses

Fig. 11 shows an intensity peak near 2θ = 22° and a minimum near 2θ = 18°. Crystallinity was measured by the index of crystallinity, which was calculated by the occupancy rate of the crystalline portion of the specimen (Isogai and Usuda 1990). This study used the Segal method (Eq. 24) to calculate the degree of crystallinity (C_{rI}) of the wooden dowel and the weld interface (Segal *et al.* 1959),

$$C_{rI} = \frac{\left(I_{002} - I_{am}\right)}{I_{002}} \times 100\% \quad (24)$$

where the integrated intensity (I_{002}) is the maximum intensity of the crystal diffraction angle near 2θ = 22° and the integrated intensity (I_{am}) is the minimum intensity of the amorphous diffraction angle near 2θ = 18°.

Some of the noticeable areas that indicated chemical changes are shown using red arrows in Fig. 11. The degrees of crystallinity for the wooden dowel and the welding interface were 19.2 and 33.6, respectively. Compared to the calculated data, the degree of crystallinity increased after the wooden dowel welding process. Both thermal pyrolysis and structural rearrangement played an important role in determining the content of the crystalline portion. The ruptured cellulose chain caused by the high temperatures resulted in a decreased crystallinity. However, some reactions improved the degree of crystallinity. The -OH group between the cellulose chains was dehydrated by a crosslinking reaction that caused the microfibril to be arranged orderly. Additionally, the amorphous region of the cellulose crystallized due to a rearrangement of the molecular chain. Pyrolysis of some of the portions of hemicellulose and lignin formed monocrystals that increased the degree of crystallinity. The same phenomena were observed in the Scanning Electron Microscopy (SEM) image shown in Fig. 12. The cellulose microfibrils were covered with the flowing matrix that was generated by the pyrolysed lignin and hemicellulose. Some fibrils are indicated by the white arrows.

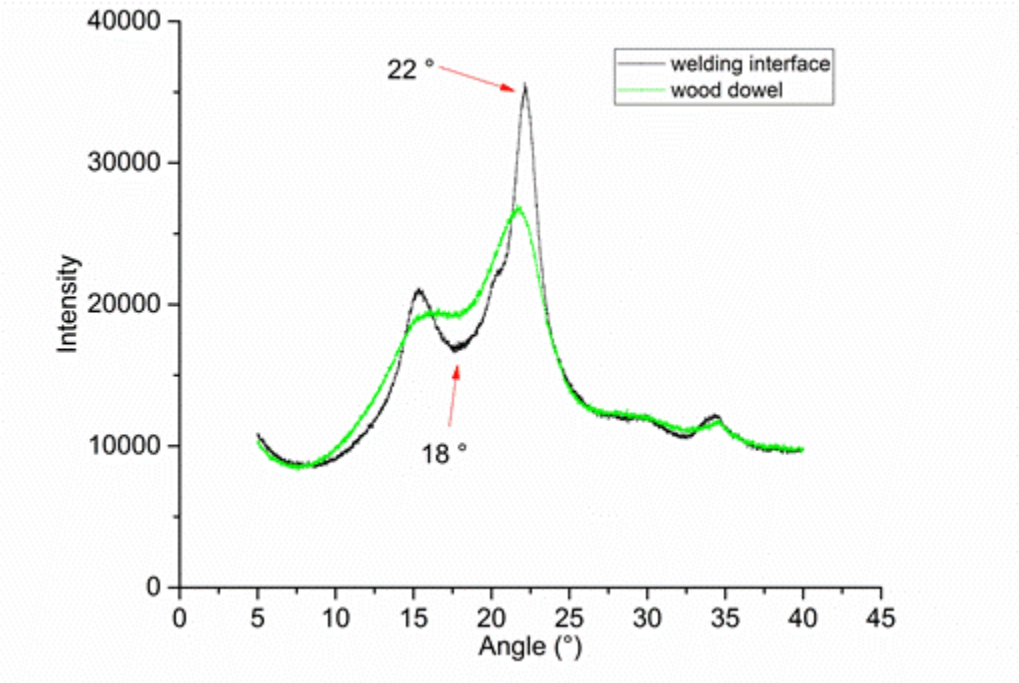

Fig. 11. XRD test of the welding interface and wooden dowel

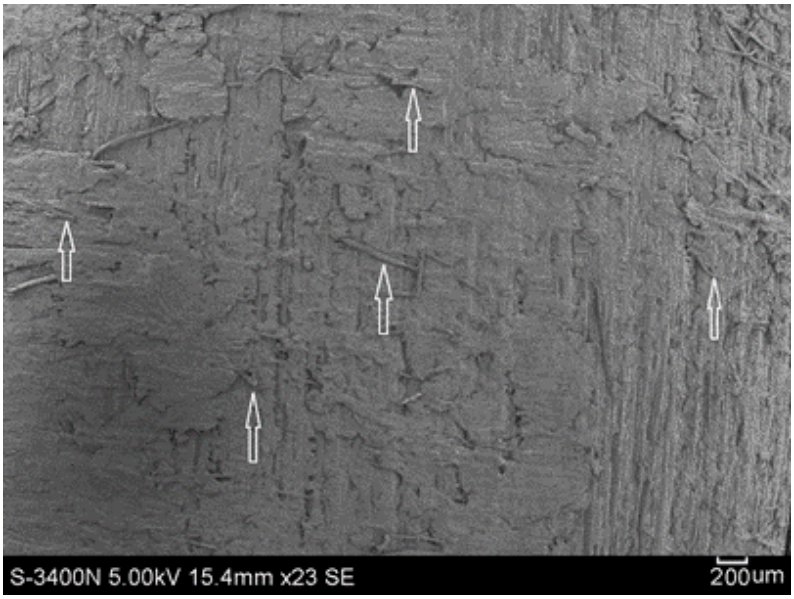

Fig. 12. Scanning electron micrograph of the welding interface

TG/DTG Analyses

The main components of wood are cellulose, hemicellulose, lignin, and a small amount of wood extractives. Under high temperature conditions, hemicellulose was the most instable. It was decomposed into polysaccharose, and further into furan derivatives. Lignin showed the best stability due to its complex reticular structure. From the TG curves seen in Fig. 8, the thermal events can be distinguished into three stages: (1) a slow weight loss below 500 K due to moisture evaporation and pyrolysis of wood extractives, (2) a major weight loss in the range of 500 K to 650 K due to the pyrolysis of cellulose, hemicellulose, and lignin, and (3) a slow and continuous weight loss at temperature above

650 K due to the decomposition of small lignin and wood extractives. During the major weight loss stage, hemicellulose decomposed in the temperature range of 500 K to 600 K, and pyrolysis of cellulose occurred in the range of 600 K to 650 K. For lignin and wood extractives, pyrolysis occurred in temperature ranges of 475 K to 775 K and 425 K to 875 K, respectively. The Fourier Transform Infrared Spectroscopy (FTIR) analyses showed that the side chains of lignin were partly pyrolyzed and the aromatic rings were stable. The 1230 cm^{-1} band decreased as the result of the pyrolysis of the phenolic hydroxyl group and methoxy group. The intensity of the two peaks at 1508 cm^{-1} and 1595 cm^{-1} increased due to the thermal condensation of the lignin, and the peak of 1460 cm^{-1} corresponded to the formation of CH_2 bridges between lignin fragments (Belleville *et al.* 2013a). After the TG testing process, the pyrolysis products of cellulose and hemicellulose were mainly volatile compounds. For lignin, pyrolysis primarily meant carbonization. Most of the lignin and wood extractives were turned into solid compounds by a high degree of aromatization and carbonization (Lu *et al*. 2004).

As shown in Fig. 13, the pyrolysis course of the welding interface was similar to that of the wooden dowel except for the final weight loss, which was lower than that of the wooden dowel. This phenomenon could be caused by the pyrolysis of cellulose and hemicellulose during the welding process, resulting in a higher relative content of lignin in the welding interface than the wooden dowel. This caused the welding interface to produce more solid compounds than the wooden dowel during the TG testing process. The pyrolysis of cellulose and hemicellulose during the welding process was evident from the DTG curves. The pyrolysis rate of the welding interface was clearly lower than that of the wooden dowel in the temperature range of 500 K to 600 K. This is likely due to the pyrolysis of hemicellulose that occurred during the welding process.

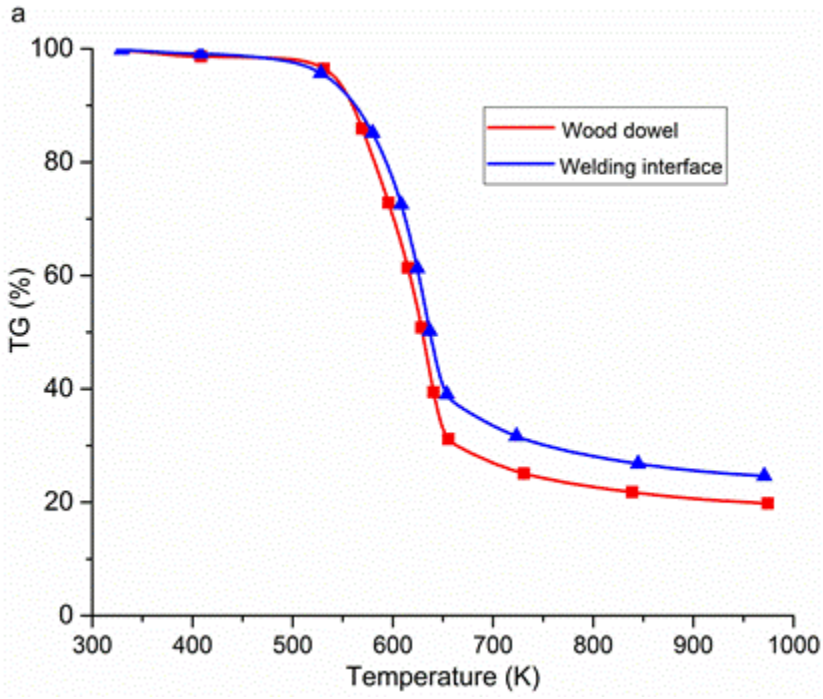

Fig. 13a. TG (a) and DTG (b) graph of the welding interface and wooden dowel

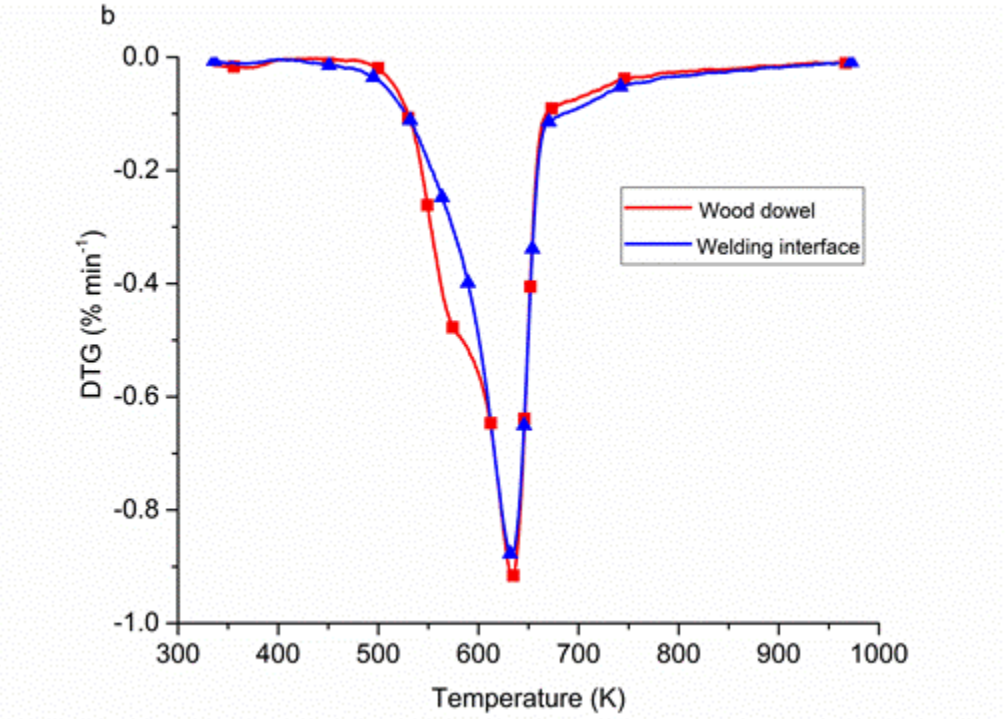

Fig. 13b. TG (a) and DTG (b) graph of the welding interface and wooden dowel

The same phenomenon was observed by Fourier Transform Infrared Spectroscopy (FTIR), and the decreased intensity of the peak at 1730 cm^{-1} corresponded to the pyrolysis of hemicellulose. At the same time, the pyrolysis rate of the welding interface was slightly lower than that of the wooden dowel around 635 K which may reflect the pyrolysis of cellulose during the welding process (Wang *et al*. 2010).

According to the above analysis, the pyrolysis degree of hemicellulose was higher than that of both the cellulose and lignin during the welding process. For lignin, few side chains were pyrolysed and the aromatic rings were stable.

CONCLUSIONS

1. Rotational welding enabled joining between the dowels and substrate with considerable strength. Group D, with a 2% MC for the wooden dowels and a 12% MC for the substrates, showed the highest pullout resistance. There was a very clear linear relationship between the pullout resistance and the different MC values. The errors between the calculated values and the test values were less than 10%.
2. The pullout resistance of the wooden dowel welding was close to the Weibull distribution. Based on the Weibull distribution, the 0.05 fractile of pullout resistance was calculated. However, no accurate linear relationship existed between the 0.05 fractile of pullout resistance and the different MC values.
3. The degree of crystallinity increased due to the recrystallization and rearrangement of the partially broken compounds after welding. From a TG/DTG analysis, the pyrolysis of cellulose and hemicellulose occurred during the welding process.

ACKNOWLEDGMENTS

The authors are grateful for the support of the Properties and Application Research of Outdoor Wood Architecture Material.

REFERENCES CITED

Auchet, S., Segovia, C., Mansouri, H. R., Meausoone, P. -J., Pizzi, A., and Omrani, P. (2010). "Accelerating *vs* constant rate of insertion in wooden dowel welding," *Journal of Adhesion Science and Technology* 24(7), 1319-1328. DOI: 10.1163/016942409X12598231568384

Belleville, B., Stevanovic, T., Cloutier, A., Pizzi, A., Prado, M., Erakovic, S., Diouf, P. N., and Royer, M. (2013a). "An investigation of thermochemical changes in Canadian hardwood species during wood welding," *European Journal of Wood and Wood Products* 71(2), 245-257. DOI: 10.1007/s00107-013-0671-x

Belleville, B., Stevanovic, T., Pizzi, A., Cloutier A., and Blanchet, P. (2013b). "Determination of optimal wood welding parameters for two North American hardwood species," *Journal of Adhesion Science and Technology* 27(5-6), 566-576. DOI: 10.1080/01694243.2012.687596

Delmotte, L., Ganne-Chedeville, C., Leban, J. M., Pizzi, A., and Pichelin, F. (2008). "CP-MAS ^{13}C NMR and FT-IR investigation of the degradation reactions of polymer constituents in wood welding," *Polymer Degradation and Stability* 93(2), 406-412. DOI: 10.1016/ j.polymdegradstab. 2007.11.020

Ganne-Chedeville, C., Pizzi, A., Thomas, A., Leban, J. M., Bocquet, J. -F., Despres, A., and Mansouri, H. (2005). "Parameter interactions in two-block welding and the wood nail concept in wooden dowel welding," *Journal of Adhesion Science and Technology* 19(13-14), 1157-1174. DOI: 10.1163/15685610577 4429037

He, F., Wang, S. F., and Yang, Y. G. (2001). "Evaluation of the dispersity of carbon fiber tensile strength by weibull theory," *Hi-Technology Fiber and Application* 26(3), 29-31.

Hu, S. Y., Zhang, Z. P., and Huang, B. Z. (1998). "Analysis of DTA/TG curve of wood flame retardant of inorganic boride series," *Journal of Fujian College of Forestry* 18, 163-166. DOI: 10.13324/j.cnki.jfcf.1998. 02.017

Isogai, A., and Usuda, M. (1990). "Crystallinity index of cellulosic materials," *Fiber* 46(8), 324-329. DOI: 10.2115/FIBER.46.8_324

Kanazawa, F., Pizzi, A., Properzi, M., Delmotte, L., and Pichelin, F. (2005). "Parameters influencing wood-dowel welding by high-speed rotation," *Journal of Adhesion Science and Technology* 19(12), 1025-1038. DOI: 10.1163/156856105774382444

Leban, J. -M., Mansouri, H. R., Omrani, P., and Pizzi, A. (2008). "Dependence of dowel welding on rotation rate," *Holz Roh Werkst* 66(3), 241-242. DOI: 10.1007/s00107-008-0228-6

Lu, W. H. (2004). *Preparation of Wood/montmorillonite (MMT) Intercalation Nanocomposite*, Ph.D. Dissertation, Beijing Forestry University, Beijing, China.

O'Loinsigh, C., Oudjene, M., Shotton, E., Pizzi, A., and Fanning, P. (2012). "Mechanical behaviour and 3D stress analysis of multi-layered wooden beams made with welded-through wooden dowels," *Composite Structure* 94(2), 313-321. DOI: 10.1016/j.compstruct. 2011.08.029

Omrani, P., Masson, E., Pizzi, A., and Mansouri, H. R. (2008). "Emission of gases and degradation volatiles from polymeric wood constituents in friction welding of wooden dowels," *Polymer Degradation and Stability* 93(4), 794-799. DOI: 10.1016/j.polymdegradstab.2008.01.017

Pizzi, A., Despres, A., Mansouri, H. R., Leban, J. -M., and Rigolet, S. (2006). "Wood joints by through-dowel rotation welding: Microstructure, ^{13}C-NMR, and water resistance," *Journal of Adhesion Science and Technology* 20(5), 427-436. DOI: 10.1163/156856106777144327

Rodriguez, G., Diouf, P., Blanchet, P., and Stevanovic, T. (2010). "Wood-dowel bonding by high-speed rotation welding-application to two Canadian hardwood species," *Journal of Adhesion Science and Technology* 24(8/10), 1423-1436. DOI: 10.1163/016942410X501025

Sandberg, D., Haller, P., and Navi, P. (2013) "Thermo-hydro and thermos-hydro-mechanical wood processing: An opportunity for future environmentally friendly wood products," *Wood Material Science & Engineering* 8, 64-88. DOI: 10.1080/17480272.2012.751935

Segal, L. C., Creely, J. J., Martin, A. E. J., and Conrad, C. M. (1959). "An empirical method for estimating the degree of crystallinity of native cellulose using the X-ray diffractometer," *Textile Research Journal* 29(10), 786-794. DOI: 10.1177/004051755902901003

Segovia, C., and Pizzi, A. (2009). "Performance of dowel-welded wood furniture linear joints," *Journal of Adhesion Science and Technology* 23(9), 1293-1301. DOI: 10.1163/156856109X 434017

Tan, H., Wang, S. R., and Luo, Z. Y. (2006). "Pyrolysis behavior of cellulose, xylan, and lignin," *Journal of Fuel Chemistry and Technology* 34, 61-65. DOI: 0253-2409(2006)01-0061-05

Wang, K. G. (2010). *Experimental Study of Lignin Pyrolysis*, Master's Thesis, Zhejiang University, Zhejiang, China.

Yi, Y. (2002). *The Statistic Analyses to the Strength of Materials*, Master's Thesis, Sichuan University, Sichuan, China.

Zheng, Y. Q., Sun, Y. J., Ding, C., Liang, H. Q. (2012). "Weibull distribution for strength of glass fiber reinforced polyamide composites," *Engineering Plastics Application* 40(7), 64-67. DOI: 10.3969/j.issn.1001-3539.2012.07.016

Zhou, X. J., Pizzi, A., and Du, G. B. (2014). "Research progress of wood welding technology (bonding without adhesive)," *China Adhesives* 23(6), 47-53.

Article submitted: December 27, 2016; Peer review completed: February 2, 2017;
Revised version received and accepted: February 27, 2017; Published: March 21, 2017.
DOI: 10.15376/biores.12.2.3396-3412